ELECTRONIC SUPPLEMENTARY MATERIAL:

ECOLOGICAL CONSTRAINTS COUPLED WITH DEEP-TIME HABITAT DYNAMICS PREDICT THE LATITUDINAL DIVERSITY GRADIENT IN REEF FISHES

Théo Gaboriau, Camille Albouy, Patrice Descombes, David Mouillot, Loïc Pellissier, Fabien Leprieur

Proceedings B

doi: 10.1098/rspb.2016.0049

SUPPLEMENTARY METHODS

Species distribution

To compare the observed patterns of reef fish biodiversity to those predicted by the process-based models, we gathered distribution data for reef fish species. We inventoried 16 238 200 occurrence records from 34883 entries in the Ocean Biogeographic Information System (OBIS, http://www.iobis.org). We cleaned the data by identifying the synonyms, misspellings and rare species (only one occurrence) and by constraining the data set to include only reef fish species from the acanthomorph group according to FishBase. Synonyms were converted to accepted names. We reconstructed distribution maps for each species, defined as the convex polygon surrounding the area where each species was observed. The resulting polygon was divided into four parts across the world to integrate discontinuity between the two hemispheres and the Atlantic and Pacific Oceans. For example, non-tropical species are distributed in the Northern and Southern Hemispheres but show a range discontinuity near the tropics (1), and a polygon division allowed accounting for this singularity. We refined each species distribution map by removing areas where maximal depths fell outside the minimum or maximum known depth range of the species. Final distribution maps of well-known species were checked visually and reviewed. As the OBIS database did not well represent the tropical assemblage of fish, we merged the database with the Gaspar database at a 1° resolution (2,3). We obtained a global database containing 4670 reef fish species that we aggregated on a 1°-resolution grid covering all oceans. We transformed individual species shapefiles into equal-area raster grids at a resolution of 1°.

Habitat reconstruction

To provide realistic predictions of reef fish biodiversity dynamics, we reconstructed the evolution of potential reef habitats through geological time. We employed an absolute plate motion model based on marine magnetic anomalies and fracture zone tracks in the crust of today's ocean basins (3,4). We generated synthetic paleobathymetry models with a 1˚ resolution for the past 140 My in 1 million-year time steps by combining oceanic paleobathymetry grids derived from paleo-oceanic crustal age grids with continental paleogeographic data (5). To account for climatic variations since the Cretaceous, we reconstructed the paleolatitudes of tropical ocean limits from reef-forming coral fossil records from PaleoDB (www.paleodb.org). We collected fossil occurrences of scleractinian corals corresponding to 31,392 occurrences (Figure S17) with a minimum number of 176 fossil occurrence per time slice and a mean of 685 fossil occurrence per time slice. We computed the 95th percentile of the paleolatitude at which corals were living to infer the latitudinal border of tropical oceans through time. By combining reconstructed shelfal areas with tropical limits, we generated 1 map per million years of tropical and temperate shallow marine habitats, favourable for reef-fish colonisation, for the last 140 My (Figure S1). Each map contained five types of cells: 1. Landmasses considered barriers to dispersion, 2. Tropical deep waters considered non-habitat cells, 3. Temperate deep waters also considered non-habitat cells, 4. Tropical shallow waters considered habitat cells, and 5. Temperate shallow waters also considered habitat cells.

Mechanisms

Dispersion. At each time step, species disperse from one habitat at time t to another habitat at time t+1. For each species, we draw a dispersion distance from a Weibull distribution of scale d. The species colonises every habitat cell at time t+1 within the range defined by the drawn dispersion distance. If 0 habitat cells lie within that range at time t+1, the species goes extinct. Note that the distances between habitat cells are not absolute distances but estimated shortest paths taking barriers into account.

Sympatric speciation. At each time step, after the dispersion phase, each species generates a descendant in each cell of its distribution with the probability p_s. The simulations presented in the main text were run under the sympatric speciation mechanism.

Allopatric speciation. This alternative mechanism of speciation is entirely dependent on habitat dynamics and species dispersion. At each time step, if a species range is separated by a soft or hard barrier and if the distance between the two patches is greater than the distance d_s, speciation happens, and the two patches form the distribution of two distinct species. In our model, the duration of a time step is constant. Thus, it is not yet possible to add the effect of differences in evolutionary speed between lineages in simulations run with the effect of allopatric speciation.

Temperate species. In the model, a species is considered temperate (i.e., adapted to a temperate climate) when it occupies at least one temperate habitat cell. Thus, when a tropical species colonises a temperate habitat cell, we hypothesise that the adaptation to a temperate climate spreads in that species' populations during the next 1-My time step.

Simulations and model selection procedure

Simulations run under the 'time-area' (TA) hypothesis

We first ran numerous simulations based on the sole effect of habitat dynamics with a broad range of parameter values ($d \in \{1,2,3,\dots,20\}, d_s \in \{1,2,3,\dots,20\}$ and $p_s \in \{1e^{-5}, 2e^{-5}, 3e^{-5}, \dots, 1e^{-4}, 2e^{-4}\}$). For each set of parameters, we ran 10 independent simulations under the allopatric (d, d_s) or sympatric (d, p_s) mode of speciation. For each simulation, we used the Bayesian information criterion (BIC) to compare observed and simulated diversity patterns (i.e., species richness and turnover)

$$BIC = log(n)k + nlog(\sum \frac{(obs_{val} - sim_{val})^2}{n})$$

with n, the number of observations, and k, the number of parameters. The BIC varies from 0 to $+\infty$ for species richness and from $-\infty$ to 0 for species turnover, with values closer to 0 indicating a better fit between the observed and simulated data. To identify the set of parameters that best explained both α- and β-diversity patterns, we adopted a hierarchical selection procedure since an approximate Bayesian computation (ABC) approach was not possible from a computational point of view. We first selected 10% of the simulations that showed the lowest BIC values for species richness (see below). Among these simulations, we considered the best simulation to be the one with the lowest BIC value for β-diversity caused by species turnover.

Using this model selection procedure, we also aimed to determine values of d, d_s and p_s that provided realistic predictions of species richness and species turnover, which could be used in subsequent simulations based on additional considerations of latitude-dependent mechanisms (see Box 1). However, due to the computation time required by the simulations, we could not explore the full parameter space to avoid suboptimal fits. Thus, we decided to use a similar basic set of dispersion and speciation parameters to run simulations under the 'tropical niche conservatism' (TNC), 'ecological limits' (EL) and 'evolutionary speed' (ES) hypotheses. Specifically, we used the parameters of the best simulation run under the sympatric ($d = 4;\ p_s = 5e^{-5}$) and allopatric ($d = 4; d_s = 9$) modes of speciation This also allowed us to interpret the predictions of the TNC, EL and ES hypotheses with the same effect of time and area (see below).

Simulations based on additional considerations of latitude-dependent mechanisms

Based on the selected set of parameters, we ran independent simulations with the addition of latitude-dependent mechanisms as postulated by the TNC, EL and ES hypotheses, with parameter values $p_a \in \{1e^{-5}, 2e^{-5}, \dots, 1e^{-4}, 2e^{-4}, \dots, 1e^{-3}\}, r_K \text{ and } r_s \in \{0.01, 0.02, \dots, 0.1, 0.2, \dots, 1\}$, which correspond to the adaptation probability, carrying capacity ratio and speciation ratio, respectively. Notably, simulations run under the TA hypothesis displayed the following parameters: $p_a = 1, r_K = 1$ and $r_s = 1$; hence, the simulations considered the sole influence of habitat dynamics. For each set of parameters, we ran 10 independent simulations. To evaluate the predictions of each hypothesis, we followed the hierarchical selection procedure based on the BIC, as described above.

Due to the computation time required by the simulations, we could not use an ABC approach to select the simulation that best predicted species richness and species turnover simultaneously. Specifically, this approach allows for the exploration of the full parameter space to avoid potential suboptimal fits. To explore this issue, we compared the R^2 of the best simulation based on our hierarchical selection procedure to the R^2 of the best simulation for species richness and species turnover separately (i.e., the highest R^2 for species richness among all the simulations and the highest R^2 for species turnover among all the simulations). The results showed that our model selection procedure avoided the selection of simulations with suboptimal fits, i.e., the selected simulation for each model provided predictions of

richness and turnover very similar to the best prediction that could be reached for both variables (Figure S8).

SUPPLEMENTARY RESULTS AND DISCUSSION

Simulations run with allopatric speciation

Biodiversity gradients

Simulations run under the allopatric mechanism of speciation resulted in predictions of species richness similar to those under the sympatric mode of speciation. The main difference between the simulations under the mechanisms of speciation was the heterogeneity in the LDG under the allopatric mechanism of speciation and the lower predicted species richness (Figure S3, S10). These simulations predicted low levels of species richness at low latitudes and a peak of biodiversity at 45° north under the effect of habitat dynamics alone. The fit between observed and predicted species richness was good with the allopatric mechanism but lower with the sympatric mechanism (Fig S4-5). However, we observed that the allopatric mode of speciation yielded better predictions of species richness when the effect of habitat dynamics was associated with tropical niche conservatism. We did not observe clear differences between latitudinal breaks in β-diversity predicted under the two mechanisms (Figure S11).

Diversification rates

The allopatric mechanism of speciation generates higher rates of speciation and extinction than the sympatric mechanism (Figure 3, S12). Overall, the differences between rates of tropical vs. temperate lineages are of the same magnitude under the allopatric mechanism. The dynamics of speciation rates are also different between the simulations under the sympatric and allopatric modes of speciation. For instance, in the allopatric simulations, we did not observe a peak of tropical lineage speciation rates during the early Neogene. Conversely, a decline in tropical lineages beginning at the end of the Cretaceous was observed.

Effect of sympatric vs. allopatric speciation

With both speciation mechanisms, the effect of large areas of habitat on species richness could be generated by very simple neutral mechanisms that influence diversification rates. Widespread continuous habitat allows species to disperse into large ranges. Species with larger ranges then have fewer chances of facing a total loss of their reachable suitable habitat, which would lead to extinction. Species that colonised a large area of habitat also had more chances to face an event of speciation within their occupied cells and more chances to be separated by a newly originated barrier that can cause allopatric speciation. This effect gives, however, different predictions depending on the mechanism of speciation used. Under the sympatric speciation mechanism, the only determinant of the probability of speciation is the size of the species range. In its current form, our process-based model does not explicitly simulate the effect of habitat heterogeneity (6) or biotic interactions (7,8), but it considers speciation events to randomly happen inside the species range. This stochasticity generates homogeneous patterns of species richness that are not a direct consequence of the effect of barriers, habitat heterogeneity or biotic interactions. Conversely, the allopatric mechanism explicitly considers the effect of soft (e.g., deep waters) and hard (e.g., land) barriers but does not consider other potential causes of divergence. Thus, this mechanism can generate species-rich areas only at the meeting points between previously isolated regions, which leads to heterogeneous patterns of species richness. Although incomplete, we show that this mechanism generates better predictions of species turnover (Figure S2) that seem concordant with empirical data. Indeed, this high richness in secondary contact areas has been identified as a common pattern of reef fish diversity (9).

The prevalence of sympatric vs. allopatric speciation among reef fish remains highly debated (10). On the one hand, the apparent lack of barriers in the oceans allows for long-distance larval dispersion that can maintain gene flow between populations (11–14); on the other hand, many cases of allopatric speciation in the sea have been identified (9,15–17). Incorporating both mechanisms into our model probably would have provided better predictions. However, the duration of a time step (and thus an allopatric speciation event) was fixed to 1 My in our model. Consequently, we were not able to test for faster speciation (the ‘evolutionary speed’ hypothesis) with our allopatric model of speciation.

Higher rates of extinction under the allopatric model could be due to the influence of speciation events that occur in remote places (founder event speciation), which are more prone to disappear over time. With a purely sympatric mode of speciation, the probability of origination of a new species in such areas is low, leading to higher net rates of speciation and extinction.

Improving the biodiversity model

Potential limitations, such as the effect of the chosen tectonic model on our simulations, have already been addressed in previous publications using the SPLIT model (5,18). Here, we will focus on limitations that are directly linked to the mechanisms that are expected to have shaped the LDG. We invite the reader to keep in mind that, despite the good predictions of species richness and β-diversity provided by our simulations, we seek only to evaluate the potential influence of macro-evolutionary mechanisms on several patterns of biodiversity. First, as pointed out by Descombes et al. (2017), the SPLIT model can accommodate only habitat changes that occurred over large temporal scales and runs with constant time steps (here, 1 My). Thus, the effect of evolutionary speed on allopatric speciation cannot be simulated, as speciation speed cannot be modulated. Another potential limitation is the proxy we used to determine the latitude of the separation between tropical and temperate habitat. Here, we used the presence of reef-building scleractinian corals fossils as an indicator of tropical climate. First, this approach cannot capture gradual changes of sea surface temperature from the equator to the poles nor sea surface temperature differences at the same latitude due to oceanic currents. Second, this approach relies on the sampling of coral fossils. Although the fossil record for that group is abundant, there is potentially gaps in the data that could affect our estimation of the limit between tropical and temperate habitats. These caveats are expected to affect our results only at a small spatial scale as the only cells potentially affected are those at the border between temperate and tropical habitats. Furthermore, changes of latitude at the border between tropical and temperate habitats that may impact our results, are those that happen during the Neogene, the period for which we have the more fossil occurrences, and consequently a reduced bias. However, we stress that these potential caveats should always be kept in mind when using that dataset.

One of the strengths of our proposed modelling approach is that it is straightforward to add new mechanisms to the algorithm. Here, we identify several points that could be improved to correct the potential limitations and to provide a better assessment of the influence of species interactions and climatic gradients. First, changing the modelling unit from species to populations and shortening the time steps could allow several improvements. The speciation speed, extinction probability and carrying capacity of individual cells could be modulated by population size and shorter climate change events such as the Quaternary glaciations (3). Second, the addition of more precise paleoenvironmental data such as paleotemperatures could allow the introduction of continuous variations in the carrying capacity, the probability of adaptation (p_A), the probability of speciation (p_s) or the probability of extinction, as a function of paleoenvironmental gradients. Third, the model in its current form is only phenomenological and could include more mechanistic determinants of dispersion, speciation and extinction. Here, the only mechanistic determinant is habitat dynamics. One could include a more explicit influence of climatic variation, diversity dependence or species differences to test macroevolutionary hypotheses in a dynamic spatial framework.

BIBLIOGRAPHY

1. Briggs JC. Marine centres of origin as evolutionary engines. J Biogeogr. 2003;30(1):1–18.

2. Parravicini V, Kulbicki M, Bellwood DR, Friedlander a. M, Arias-Gonzalez JE, Chabanet P, et al. Global patterns and predictors of tropical reef fish species richness. Ecography (Cop) [Internet]. 2013 Dec 30 [cited 2014 Jul 16];36(12):1254–62. Available from: http://doi.wiley.com/10.1111/j.1600-0587.2013.00291.x

3. Pellissier L, Leprieur F, Parravicini V, Cowman PF, Kulbicki M, Litsios G, et al. Quaternary coral reef refugia preserved fish diversity. Science [Internet]. 2014 May 30 [cited 2014 Jul 9];344(6187):1016–9. Available from: http://www.ncbi.nlm.nih.gov/pubmed/24876495

4. Müller RD, Sdrolias M, Gaina C, Steinberger B, Heine C. Long-Term Sea-Level Fluctuations Driven by Ocean Basin Dynamics. Science (80-). 2008;319(2008):1357–62.

5. Leprieur F, Descombes P, Gaboriau T, Cowman PF, Parravicini V. Plate tectonics drive tropical

reef biodiversity dynamics. Nat Commun. 2016;7(May):11461.

6. Tornabene L, Valdez S, Erdmann M, Pezold F. Support for a ‘ Center of Origin ’ in the Coral Triangle : cryptic diversity , recent speciation , and local endemism in a diverse lineage of reef fishes (Gobiidae : Eviota). Mol Phylogenet Evol [Internet]. 2014;(82):200–10. Available from: http://dx.doi.org/10.1016/j.ympev.2014.09.012

7. Alfaro ME, Santini F, Brock CD. Do reefs drive diversification in marine teleosts? Evidence from the pufferfish and their allies (order tetraodontiformes). Evolution (N Y). 2007;61(9):2104–26.

8. Litsios G, Pearman PB, Lanterbecq D, Tolou N, Salamin N. The radiation of the clownfishes has two geographical replicates. Bellwood D, editor. J Biogeogr [Internet]. 2014 Nov 17 [cited 2014 Nov 20];41(11):2140–9. Available from: http://doi.wiley.com/10.1111/jbi.12370

9. Gaboriau T, Leprieur F, Mouillot D, Hubert N. Influence of the geography of speciation on current patterns of coral reef fish biodiversity across the Indo-Pacific. 2017;

10. Cowman PF. Historical factors that have shaped the evolution of tropical reef fishes: a review of phylogenies, biogeography, and remaining questions. Front Genet [Internet]. 2014 Nov 13 [cited 2014 Nov 14];5(November):1–15. Available from: http://www.frontiersin.org/Evolutionary_and_Population_Genetics/10.3389/fgene.2014.00394/abstract

11. Bowen BW, Rocha L a, Toonen RJ, Karl S a. The origins of tropical marine biodiversity. Trends Ecol Evol [Internet]. 2013 Jun [cited 2014 Aug 2];28(6):359–66. Available from: http://www.ncbi.nlm.nih.gov/pubmed/23453048

12. Hodge JR, Read CI, Bellwood DR, van Herwerden L. Evolution of sympatric species: a case study of the coral reef fish genus Pomacanthus (Pomacanthidae). Rocha L, editor. J Biogeogr [Internet]. 2013 Sep [cited 2014 Oct 6];40(9):1676–87. Available from: http://doi.wiley.com/10.1111/jbi.12124

13. Luiz OJ, Madin JS, Robertson DR, Rocha L a, Wirtz P, Floeter SR. Ecological traits influencing

range expansion across large oceanic dispersal barriers: insights from tropical Atlantic reef fishes. Proc Biol Sci [Internet]. 2012 Mar 7 [cited 2014 Oct 17];279(1730):1033–40. Available from: http://www.pubmedcentral.nih.gov/articlerender.fcgi?artid=3259933&tool=pmcentrez&rendertype=abstract

14. Rocha LA, Bowen BW. Speciation in coral-reef fishes. J Fish Biol. 2008;72(5):1101–21.

15. Gaither MR, Rocha L a. Origins of species richness in the Indo-Malay-Philippine biodiversity hotspot: evidence for the centre of overlap hypothesis. Dawson M, editor. J Biogeogr [Internet]. 2013 Sep 29 [cited 2014 Nov 12];40(9):1638–48. Available from: http://doi.wiley.com/10.1111/jbi.12126

16. Quenouille B, Hubert N, Bermingham E, Planes S. Speciation in tropical seas: Allopatry followed by range change. Mol Phylogenet Evol [Internet]. 2011 Mar [cited 2014 Sep 27];58(3):546–52. Available from: http://www.ncbi.nlm.nih.gov/pubmed/21256237

17. Hubert N, Meyer CP, Bruggemann HJ, Guérin F, Komeno RJL, Espiau B, et al. Cryptic diversity in indo-pacific coral-reef fishes revealed by DNA-barcoding provides new support to the centre-of-overlap hypothesis. PLoS One [Internet]. 2012 Jan [cited 2014 Sep 27];7(3):e28987. Available from: http://www.pubmedcentral.nih.gov/articlerender.fcgi?artid=3305298&tool=pmcentrez&rendertype=abstract

18. Descombes P, Gaboriau T, Albouy C, Heine C, Leprieur F, Pellissier L. Linking species diversification to palaeo-environmental changes: A process-based modelling approach. Glob Ecol Biogeogr [Internet]. 2017;00(December):1–12. Available from: http://doi.wiley.com/10.1111/geb.12683

19. Sunday J, Bates A, Dulvy N. Nature climate change. [Internet]. Nature Climate Change. Nature Pub. Group; 2012 [cited 2018 Oct 26]. 1–5 p. Available from: http://ecite.utas.edu.au/78341

20. Rabosky DL, Chang J, Title PO, Cowman PF, Sallan L, Friedman M, et al. An inverse latitudinal

gradient in speciation rate for marine fishes. Nature [Internet]. 2018 Jul 4 [cited 2018 Aug 24];559(7714):392–5. Available from: http://www.nature.com/articles/s41586-018-0273-1

Supplementary figures

Figure S1: Examples of habitat layers used in the simulation for different periods of time.

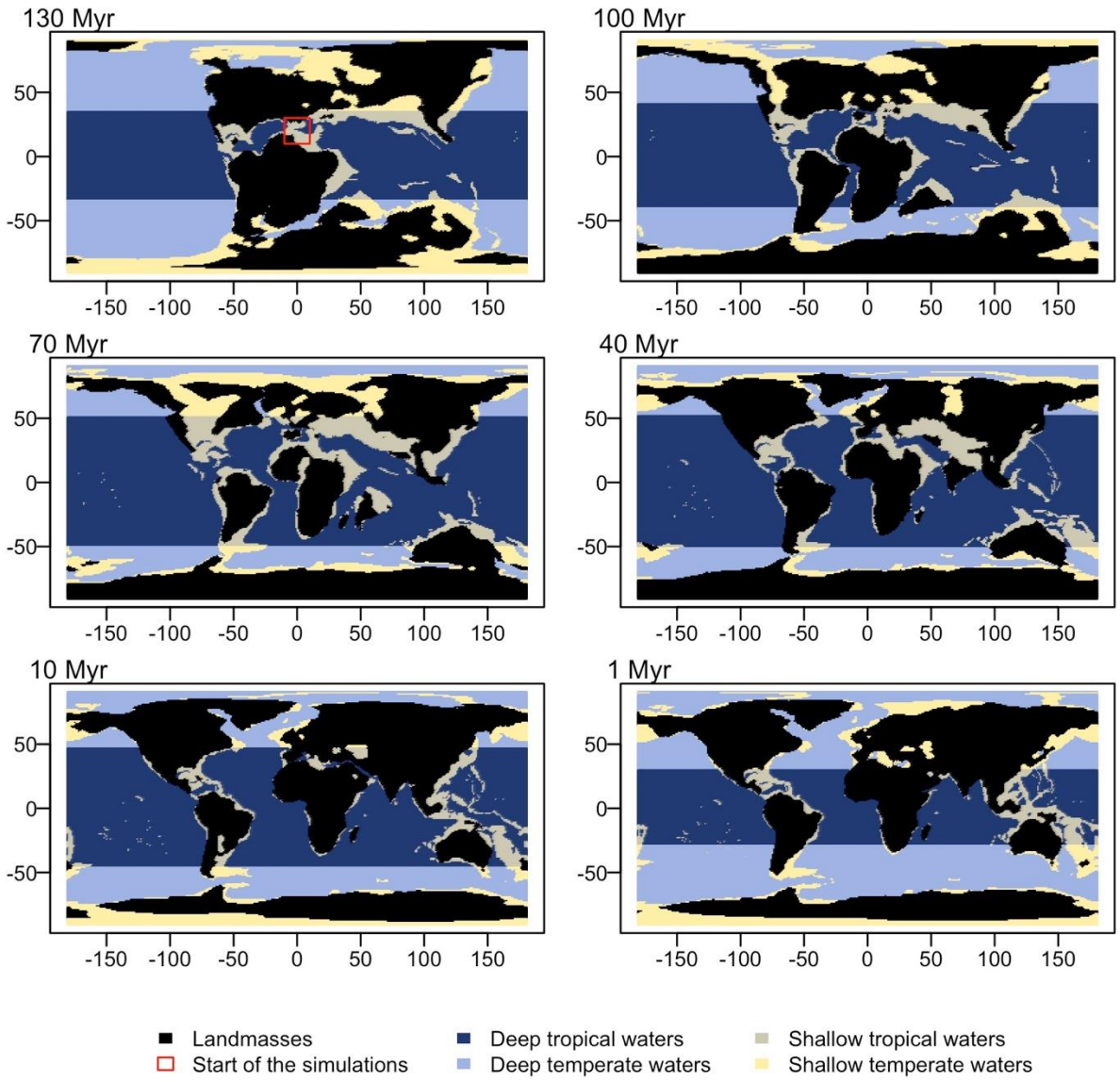

Table S1. Detection of breakpoints in species richness along the latitudinal gradient for the best simulation of each model (TA, time-area; EL, ecological limits; TNC, tropical niche conservatism; and ES, evolutionary speed). We performed piecewise regressions based on the Akaike information criterion (AIC) to test for the existence of latitudinal breakpoints in species richness. We separated the Atlantic and Indo-Pacific regions to perform those analyses. The table shows the ΔAIC for varying numbers of breakpoints as well as estimates of the breakpoint position in degrees of latitude (°) for the piecewise regression model with a ΔAIC<2. Observed: results of the piecewise regression based on the empirical dataset.

	ΔAIC				**Estimates**				
	0 break	1 break	2 breaks	3 breaks	p-value (slope)	R^2	break 1	break 2	break 3
Indo-Pacific									
Observed	376.1	136.2	75.3	0	<2e-16	0.96	-17.9	23.7	43.2
TA	244.8	91.8	8.9	0	<2e-16	0.91	-22.1	45.8	47.4
EL	361.3	113.1	62.6	0	<2e-16	0.96	-18.5	23.3	36.1
TNC	33.3	92.9	54.1	0	<2e-16	0.95	-17.6	22.6	35
ES	323.3	176.9	77.6	0	<2e-16	0.95	-23.4	45.8	47.2
Atlantic									
Obs.	310.8	103.5	33.7	0	<2e-16	0.95	4	23.5	41.2
TA	38.3	0	1.22	-0.17	0.03	0.44	17.6	-	-
EL	237.6	66.5	48.7	0	<2e-16	0.89	-21	28.6	37.1
TNC	216.7	56.6	34.3	0	<2e-16	0.88	-1.5	30.1	36.8
ES	95.8	8.8	2.4	0	3.06e-09	0.60	2.9	40.4	51.8

Figure S2: Observed and simulated patterns of β-diversity caused by species turnover. The simulated pattern is shown for the best simulation of the ecological limits (EL) (ecological limits) model ($d = 4; p_s = 5e^{-5}; r_K = 0.1; R^2 = 0.38$). For each region, we projected the pairwise dissimilarity matrix based on β_{jtu} into a two-dimensional space using non-metric dimensional scaling, and we assigned a colour to each cell depending on its position on the two-dimensional space.

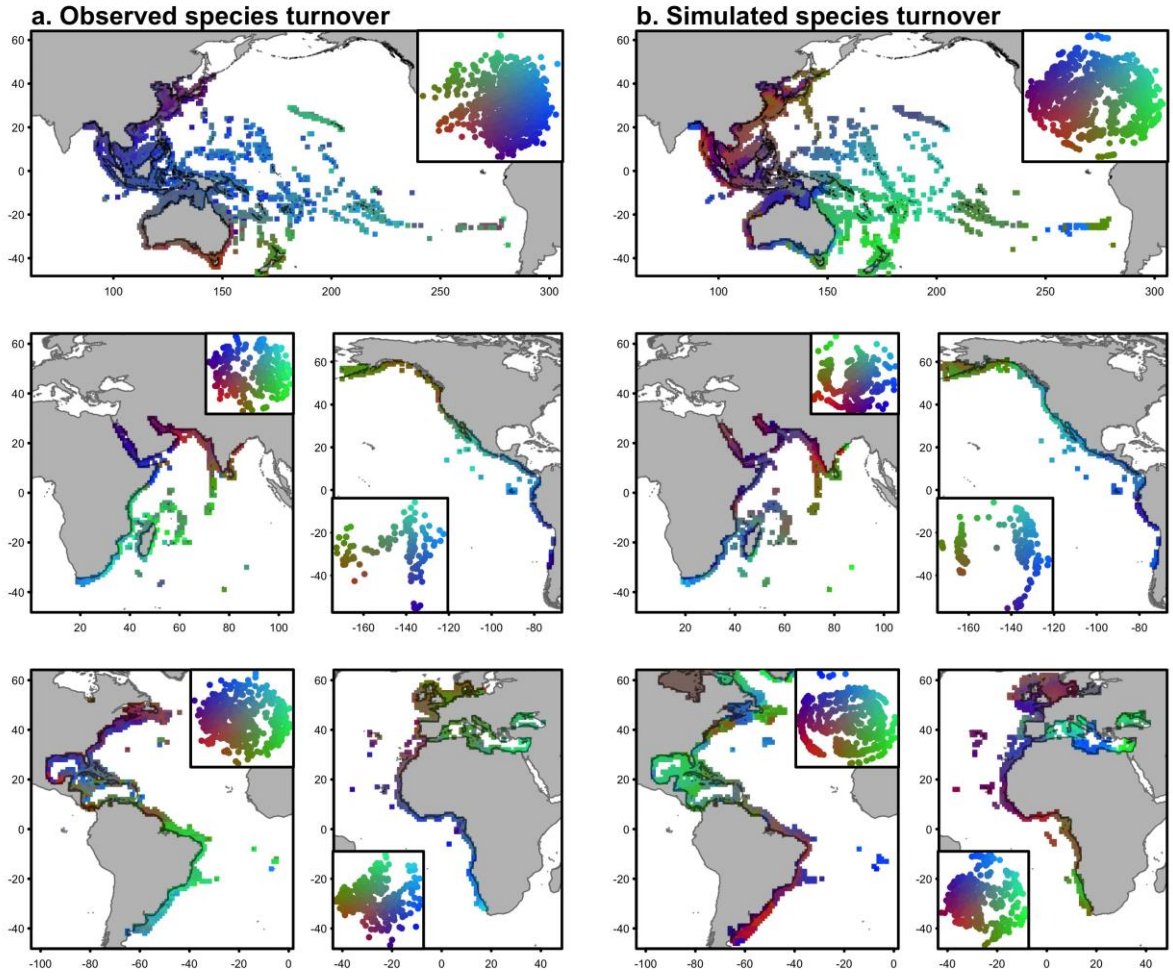

Figure S3. Simulated species richness for the best simulations run under each model. **a.** Time-area (TA) model, **b.** tropical niche conservatism (TNC) model, **c.** ecological limits (EL) model and **d.** evolutionary speed (ES) model. The left panels show simulations run under the sympatric mode of speciation, while the right panels show simulations run under the allopatric mode of speciation. The colours are scaled based on the range of values of observed reef fish species richness.

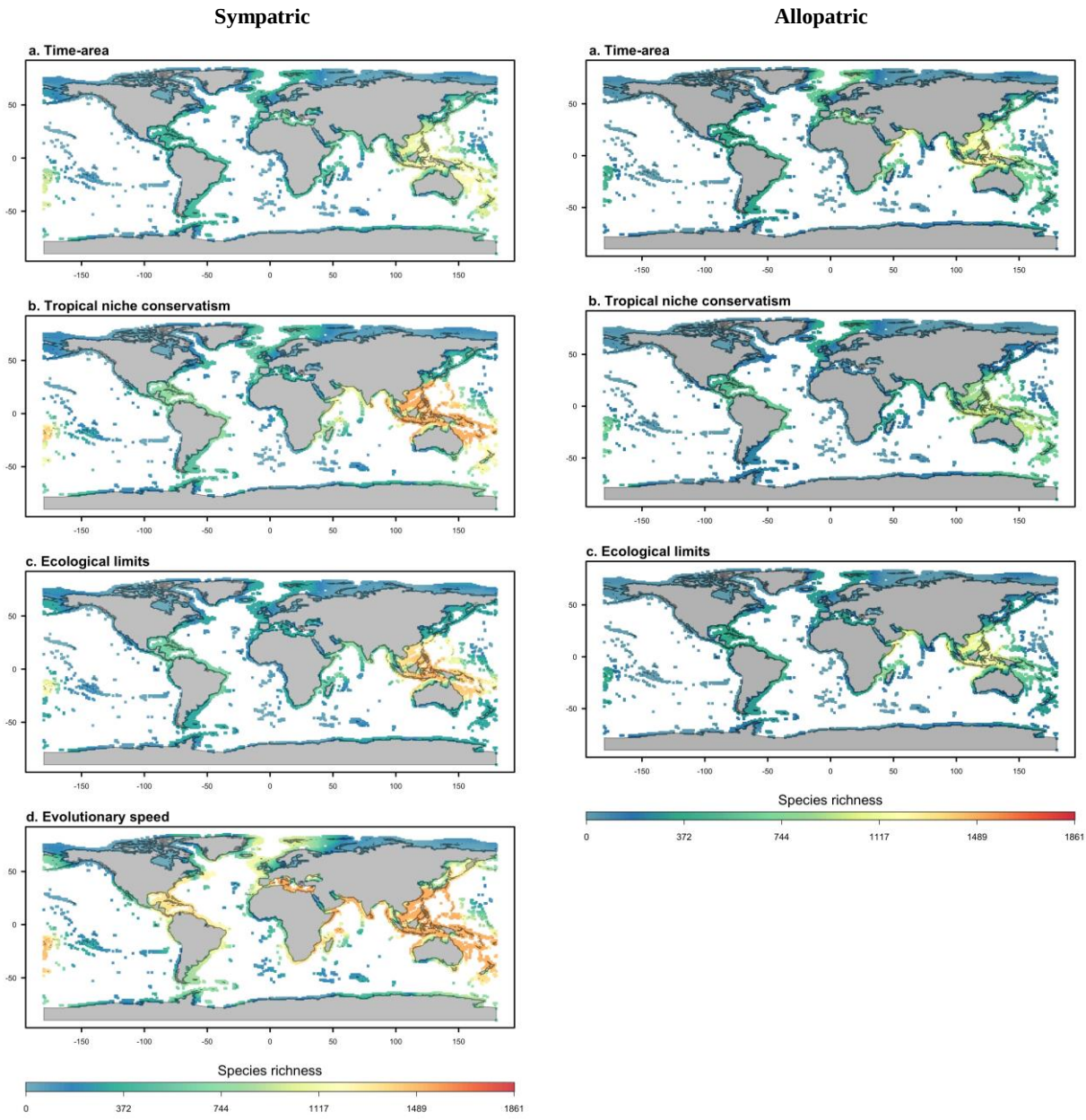

Figure S4. BIC comparisons for the models run under the 'tropical niche conservatism', 'ecological limits' and 'evolutionary speed' hypothesis with a sympatric mode of speciation ($d = 4$; $p_s = 5e^{-5}$). Estimated BIC for species richness and species turnover for each model under a wide range of parameters. p_a: Probability of adaptation when a tropical species colonises a temperate habitat. r_K: Ratio of the carrying capacity between temperate and tropical habitats. r_s: Ratio of the speciation rate between temperate and tropical habitats. In each panel, the black dot corresponds to simulations run under the 'time area' model (TA, $p_a = 1$; $r_K = 1$; $r_s = 1$). The first row of panels presents the BIC for species richness, and the second row presents the BIC for species turnover.

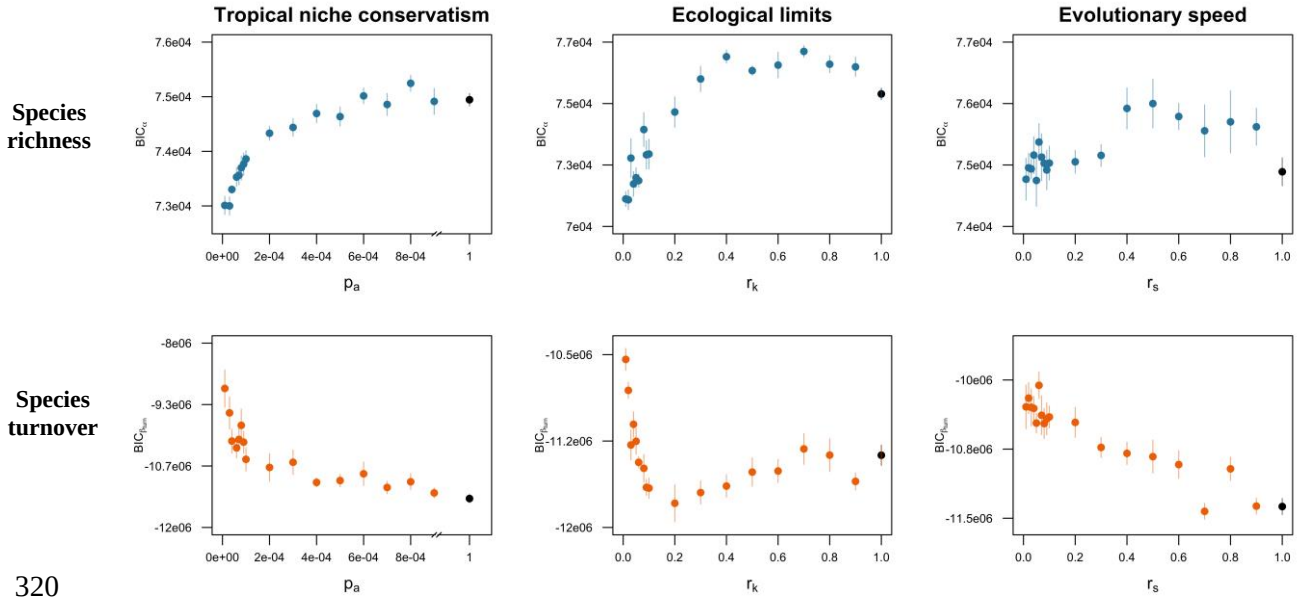

Figure S5. BIC comparisons for the models run under the 'tropical niche conservatism', 'ecological limits' and 'evolutionary speed' hypothesis with the allopatric mode of speciation ($d = 4$; $d_s = 9$). Estimated BIC for species richness and species turnover for each model under a wide range of parameters. p_a: Probability of adaptation when a tropical species colonises a temperate habitat. r_K: Ratio of the carrying capacity between temperate and tropical habitats. In each panel, the black dot corresponds to simulations run under the 'time area' model (TA, $p_a = 1$; $r_K = 1$). The first row of panels presents the BIC for species richness, and the second row presents the BIC for species turnover.

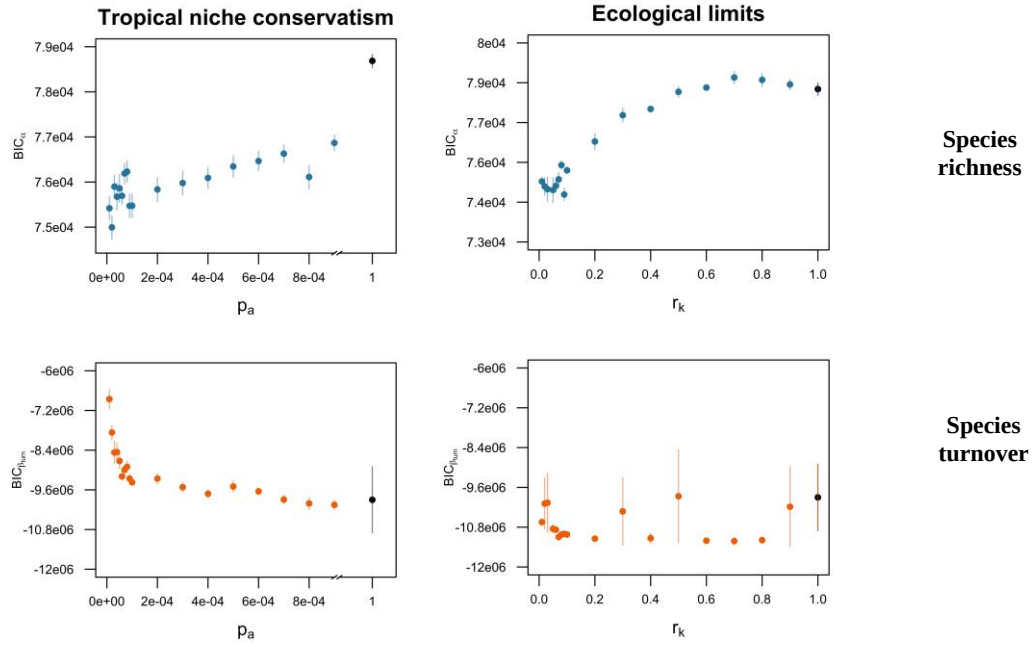

Figure S6. R^2 comparisons for the models run under the 'tropical niche conservatism', 'ecological limits' and 'evolutionary speed' hypothesis with the sympatric mode of speciation ($d = 4$; $p_s = 5e^{-5}$). Estimated R^2 for species richness and species turnover for each model under a wide range of parameters. p_a: Probability of adaptation when a tropical species colonises a temperate habitat. r_K: Ratio of the carrying capacity between temperate and tropical habitats. r_s: Ratio of the speciation rate between temperate and tropical habitats. In each panel, the black dot corresponds to simulations run under the 'time area' model (TA, $p_a = 1$; $r_K = 1$; $r_s = 1$). The first row of panels presents the R^2 for species richness, and the second row presents the R^2 for species turnover.

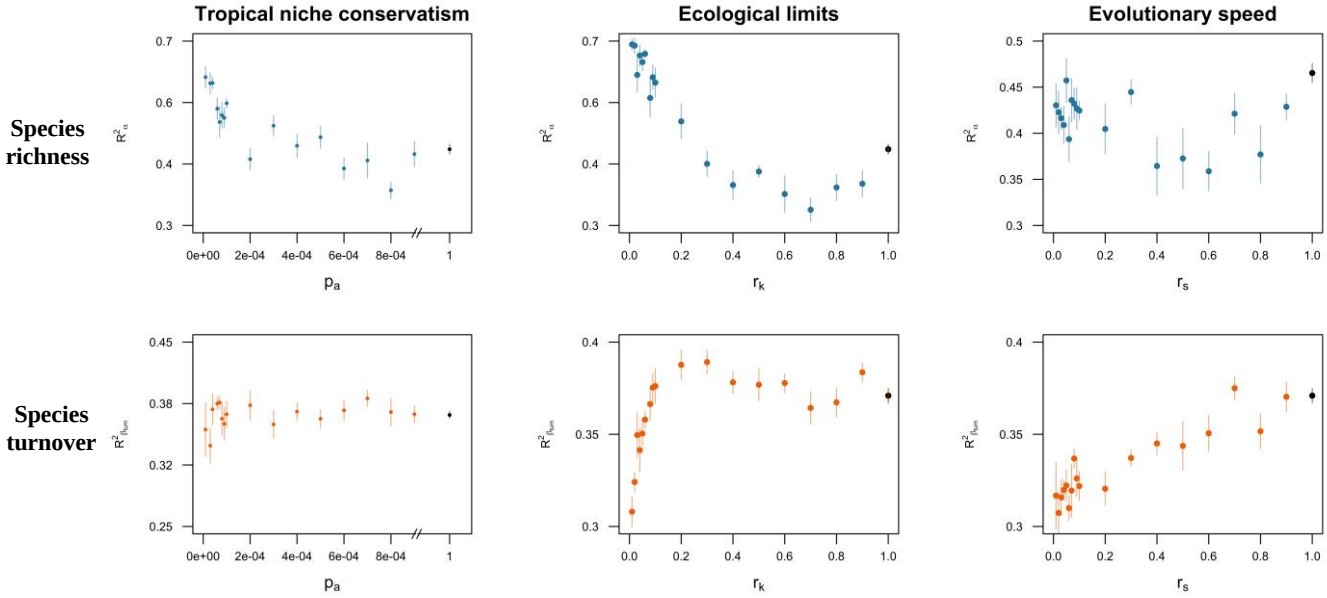

Figure S7. R^2 comparisons for the models run under the 'tropical niche conservatism', 'ecological limits' and 'evolutionary speed' hypothesis with the allopatric mode of speciation ($d = 4$; $d_s = 9$). Estimated R^2 for species richness and species turnover for each model under a wide range of parameters. p_a: Probability of adaptation when a tropical species colonises a temperate habitat. r_K: Ratio of the carrying capacity between temperate and tropical habitats. In each panel, the black dot corresponds to simulations run under the 'time area' model (TA, $p_a = 1$; $r_K = 1$). The first row of panels presents the R^2 for species richness, and the second row presents the R^2 for species turnover.

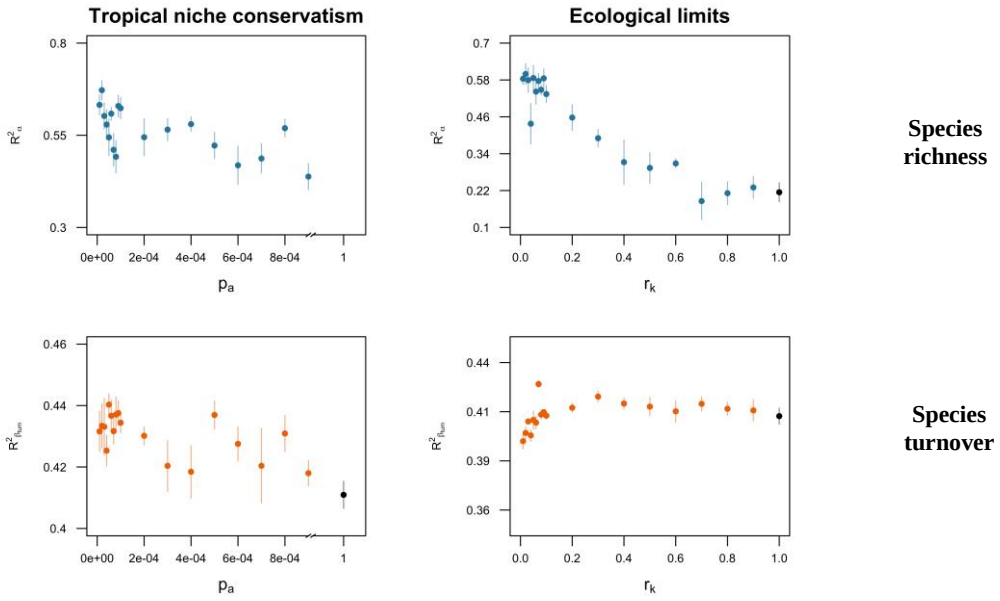

Figure S8. Efficiency of the hierarchical selection procedure based on the BIC. For each model, we compared the R^2 (observed vs. simulated species richness and species turnover) of the best simulation selected with the BIC procedure to the highest R^2 among all the simulations. Left panel: Sympatric speciation, right panel: allopatric speciation. TA: Time-area, TNC: tropical niche conservatism, EL: ecological limits, ES: evolutionary speed.

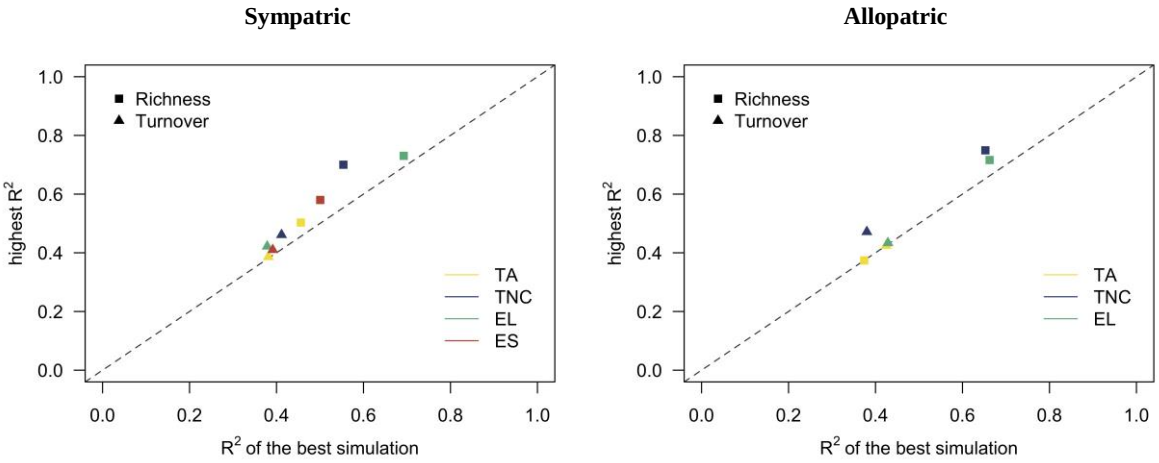

Figure S9. Latitudinal variation in beta diversity caused by species turnover through time according to the sympatric speciation model under a**.** the TA model, **b.** the TNC model, **c.** the EL model and **d.** the ES model. For the best simulation under each model, we calculated the latitudinal turnover (species turnover between each 1° cell and its adjacent cell to the north) at each time step. We then plotted the values predicted by the fitted cubic smoothing spline of latitudinal turnover vs. latitude at each time step.

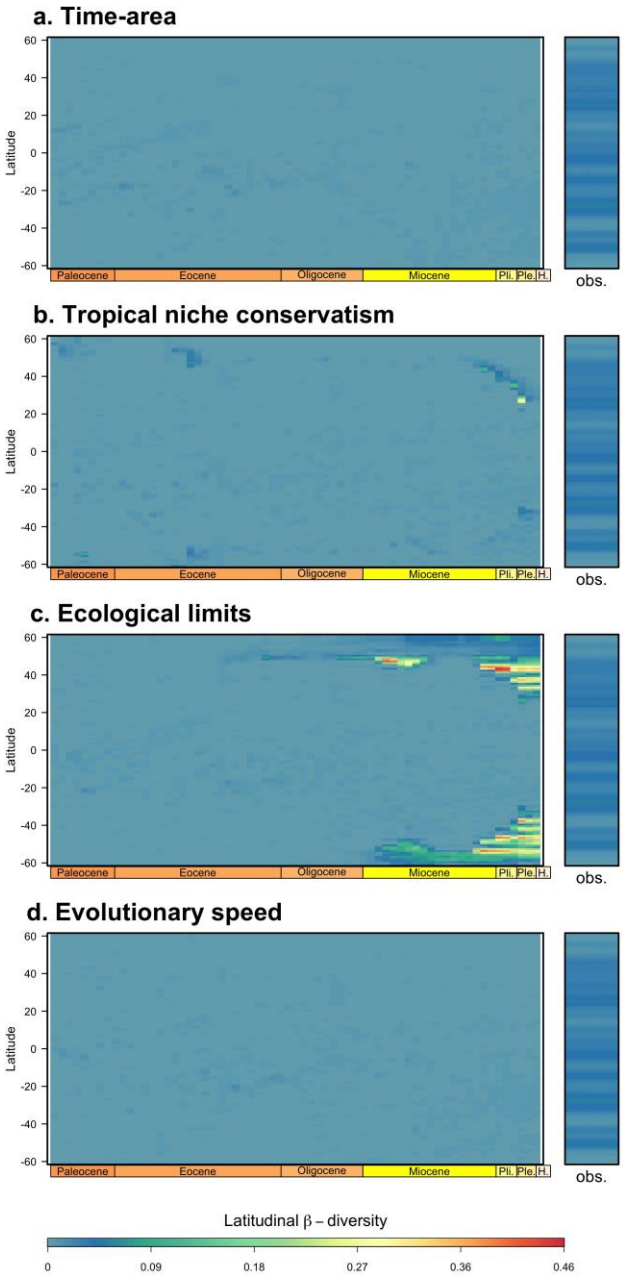

Figure S10. Evolution of the latitudinal diversity gradient in reef fishes according to simulations run with the allopatric mode of speciation: **a.** time-area (TA) model, **b.** tropical niche conservatism (TNC) model and **c.** ecological limits (EL) model. We present the latitudinal variation in reef fish species richness during geological periods from the Paleocene to the Holocene. For each mechanism, we calculated the species richness of the best simulation across latitudes at each time step. These simulated patterns can be compared to the observed latitudinal variation in species richness located on the right of each plot (obs.). *Pli*: Pliocene, *Ple*: Pleistocene, *H*: Holocene.

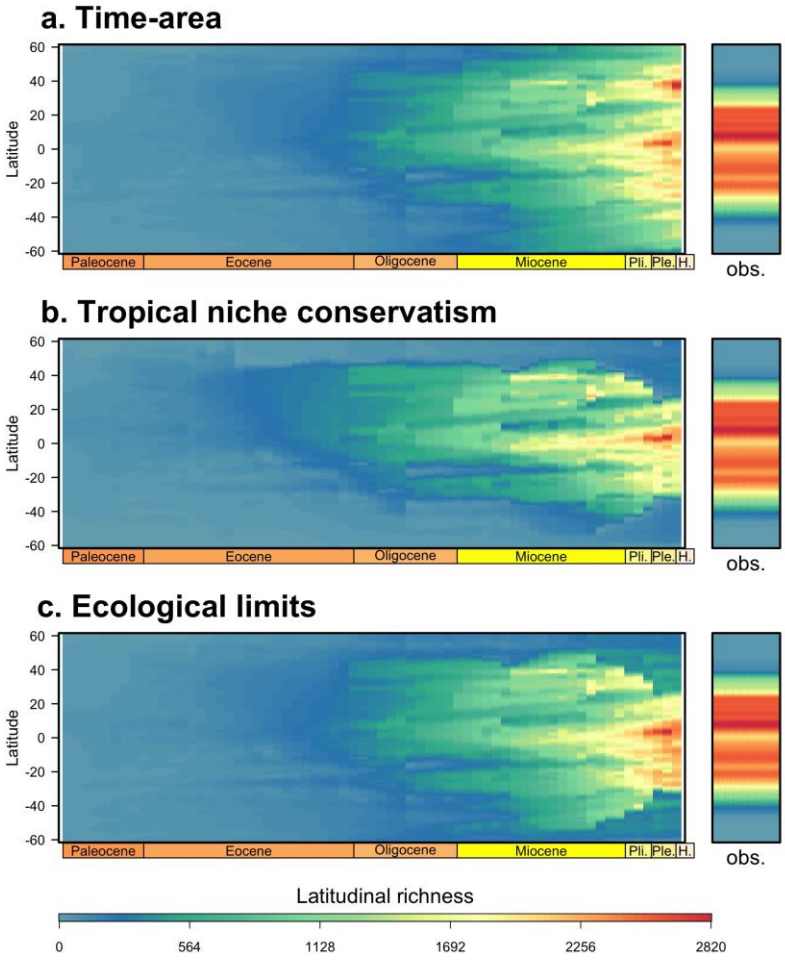

Figure S11. Latitudinal variation in beta diversity caused by species turnover through time according to the allopatric speciation model under a**.** the TA model, **b.** the TNC model, **c.** the EL model and **d.** the ES model. For the best simulation under each model, we calculated the latitudinal turnover (species turnover between each 1° cell and its adjacent cell to the north) at each time step. We then plotted the values predicted by the fitted cubic smoothing spline of latitudinal turnover vs. latitude at each time step.

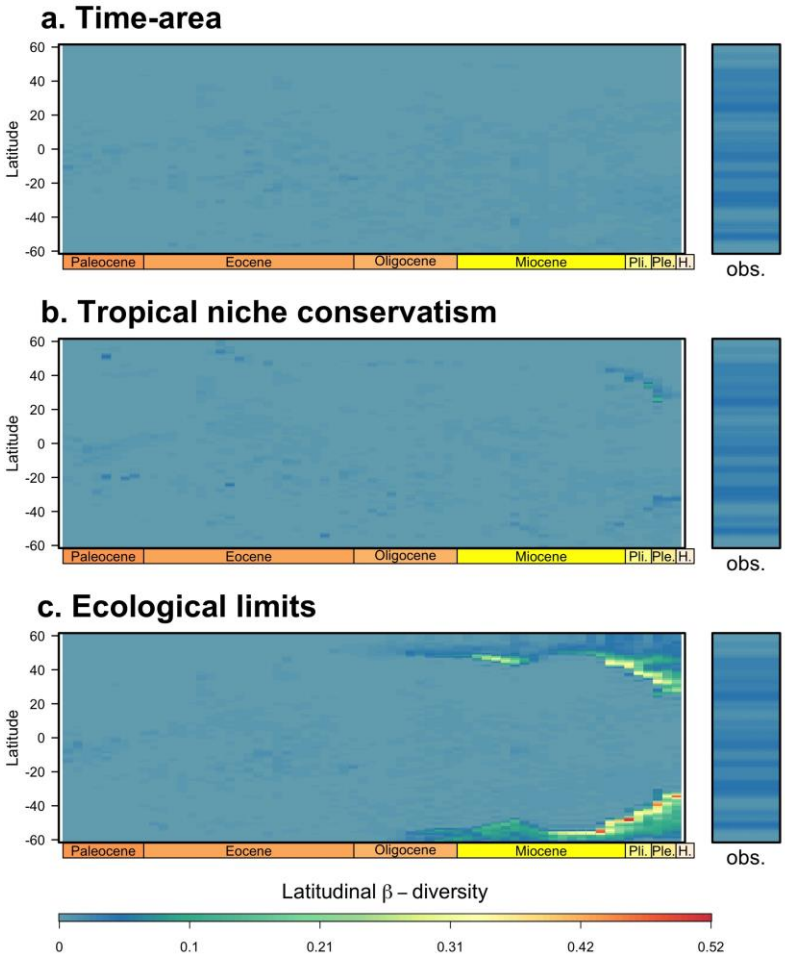

Figure S12. Diversification and dispersal rates through time under each model according to the allopatric speciation mode. We calculated the speciation, extinction and dispersion rates of tropical and temperate lineages in each simulation with time periods of 5 My. The rates were calculated as the number of events (inside and outside the tropics) divided by the number of lineages (tropical and temperate lineages, respectively) divided by the length of the time period (here, 5 My). The rates are thus expressed as events per lineage per My. Note that widespread lineages are considered both tropical and temperate. For each mechanism, we calculated the rates for the 10 simulations run with the set of parameters that rendered the best simulations. In the two first columns, red: tropical lineages, blue: temperate lineages. In the third column, red: dispersion towards the poles, blue: dispersion towards the tropics.

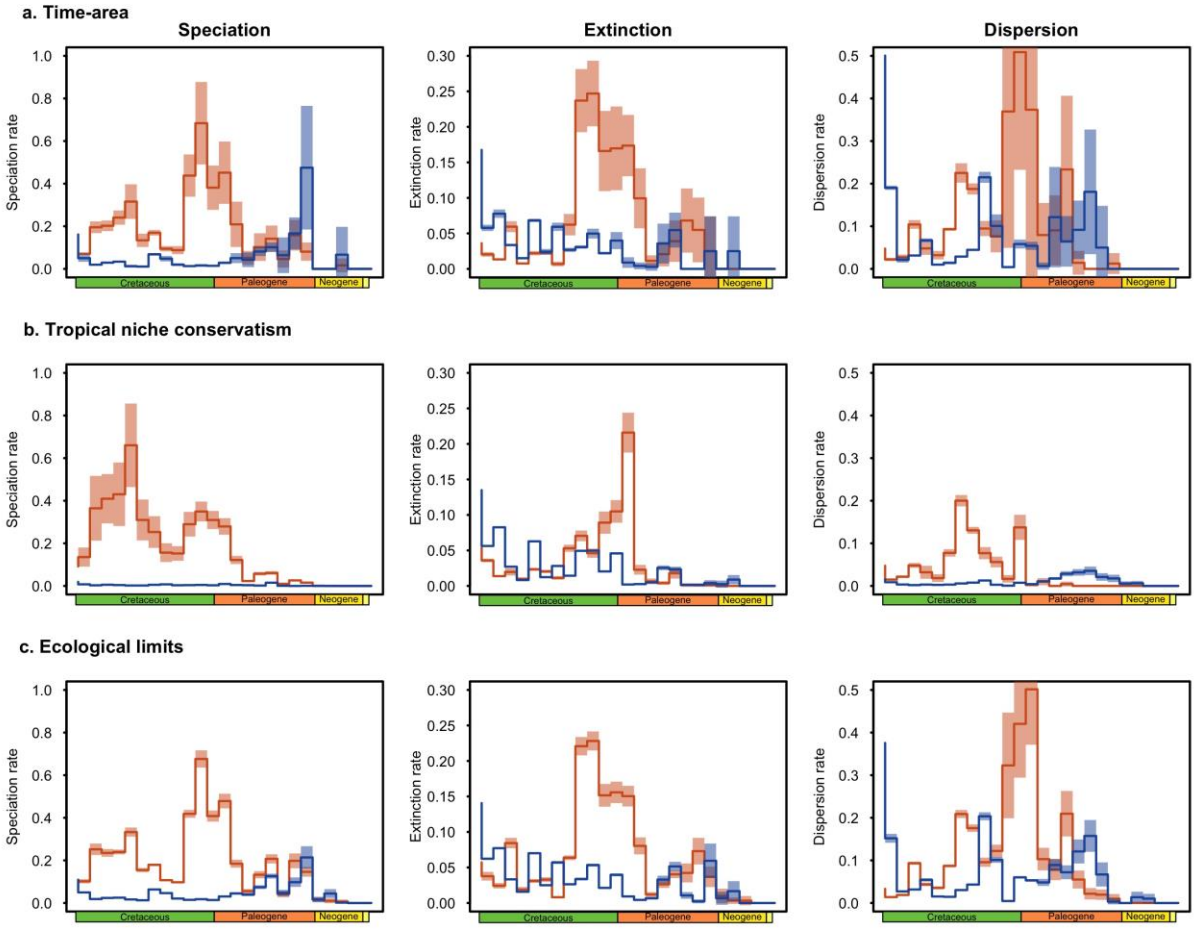

Figure S13: Evolution of potential reef habitat area through time. The red line represents the area of potential tropical reef habitat, and the blue line represents the area of potential temperate reef habitat.

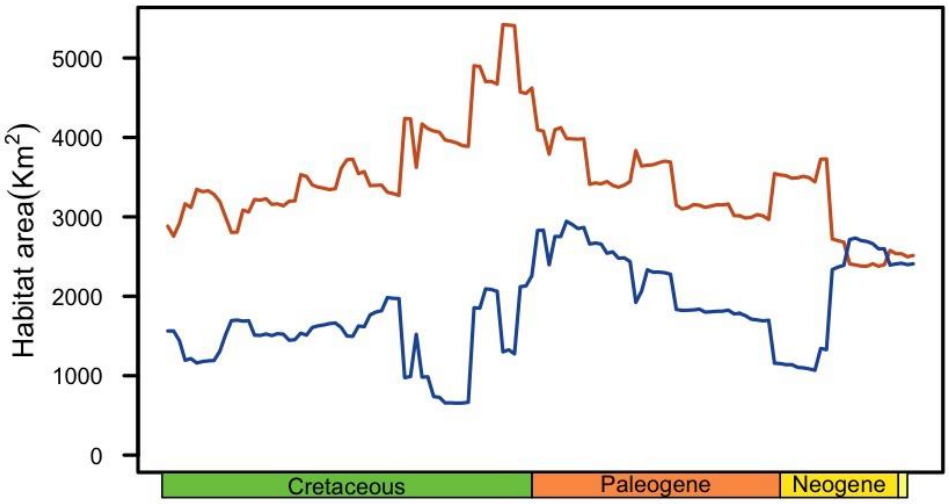

Figure S14: Evolution of the absolute latitude of the reconstructed limit between tropical and temperate habitats.

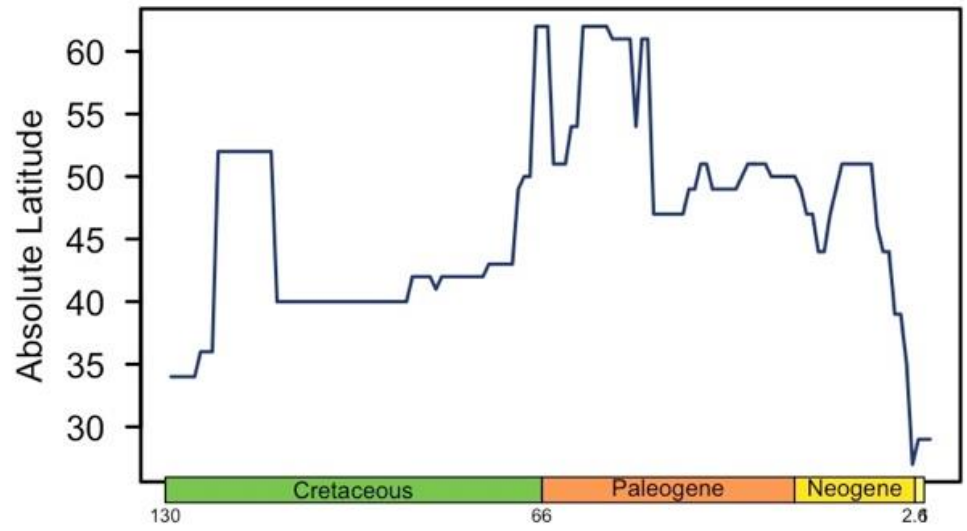

Figure S15. Diversification rates through time under each model according to the sympatric (left) and allopatric (right) speciation modes. We calculated the speciation and extinction rates of tropical and temperate lineages in each simulation with time periods of 5 My. We then plotted the difference between them. The rates were calculated as the number of events (inside and outside the tropics) divided by the number of lineages (tropical and temperate lineages, respectively) divided by the length of the time period (here, 5 My). The rates are thus expressed as event per lineage per My. Note that widespread lineages were considered both tropical and temperate. For each mechanism, we calculated the rates for the 10 simulations run with the set of parameters that rendered the best simulations. In the two first columns, red: tropical lineages, blue: temperate lineages. In the third column, red: dispersion towards the poles, blue: dispersion towards the tropics.

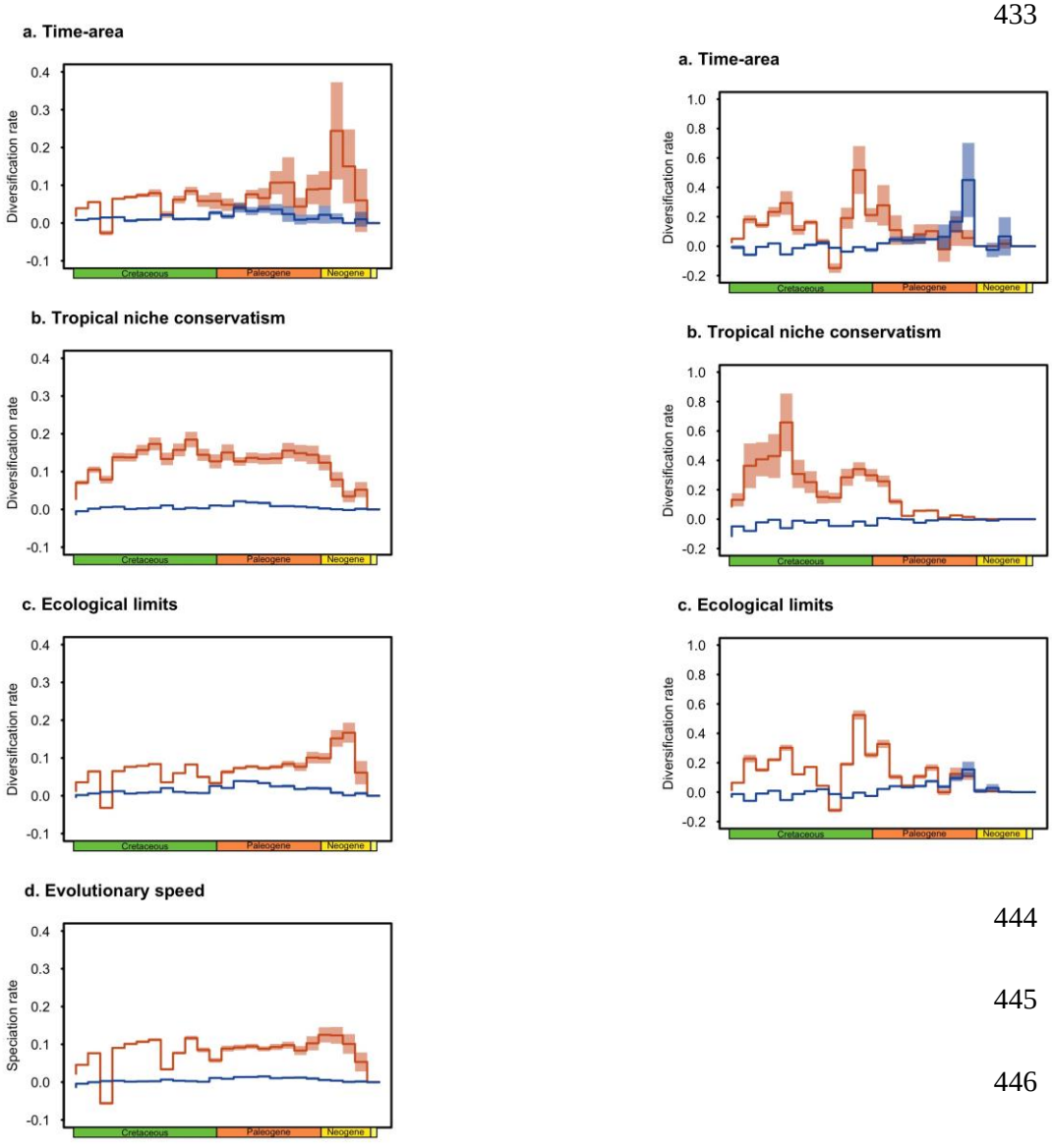

Figure S16. Global map of mean speciation rates for acanthomorph reef fish species considered in this study. We obtained recent speciation rates (λ_{bamm}) from Rabosky *et al.* (20) using the R-package *fishtree*. We calculated the weighted mean of recent speciation rates of co-occurring species in every cell (20).

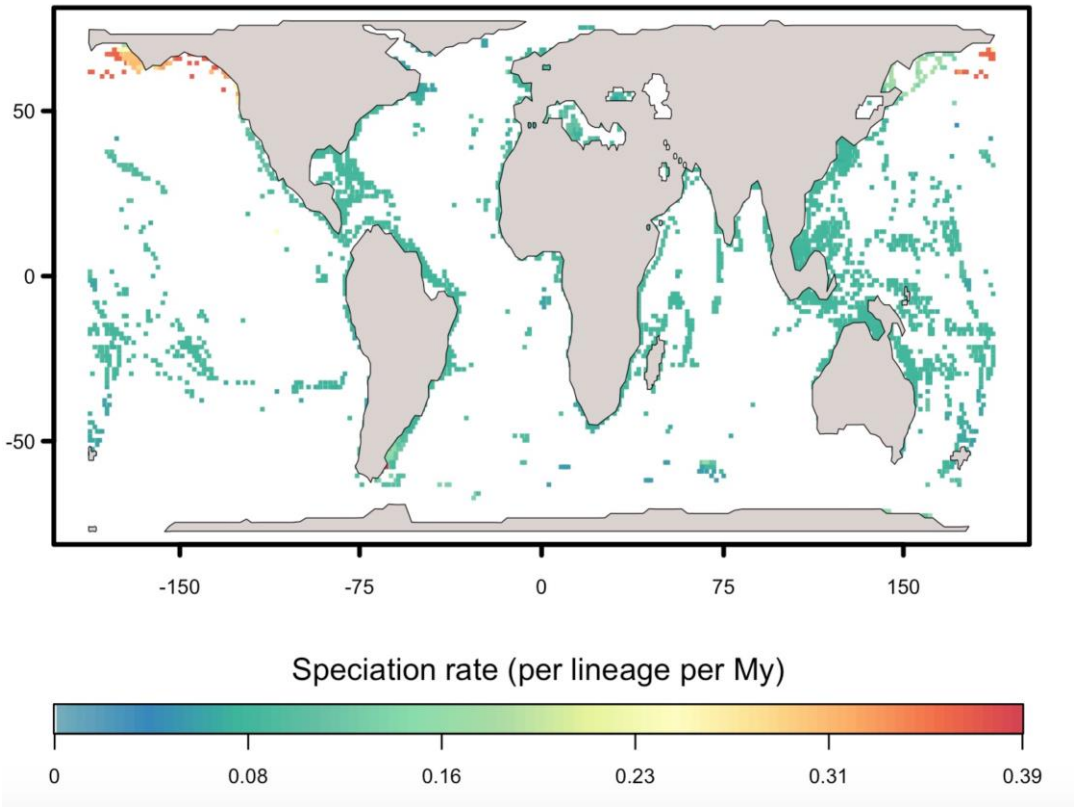

Figure S17. Map of coral fossils occurrences by period. Green: Cretaceous, Orange: Paleogene, Yellow: Neogene, Light yellow: Pleistocene.